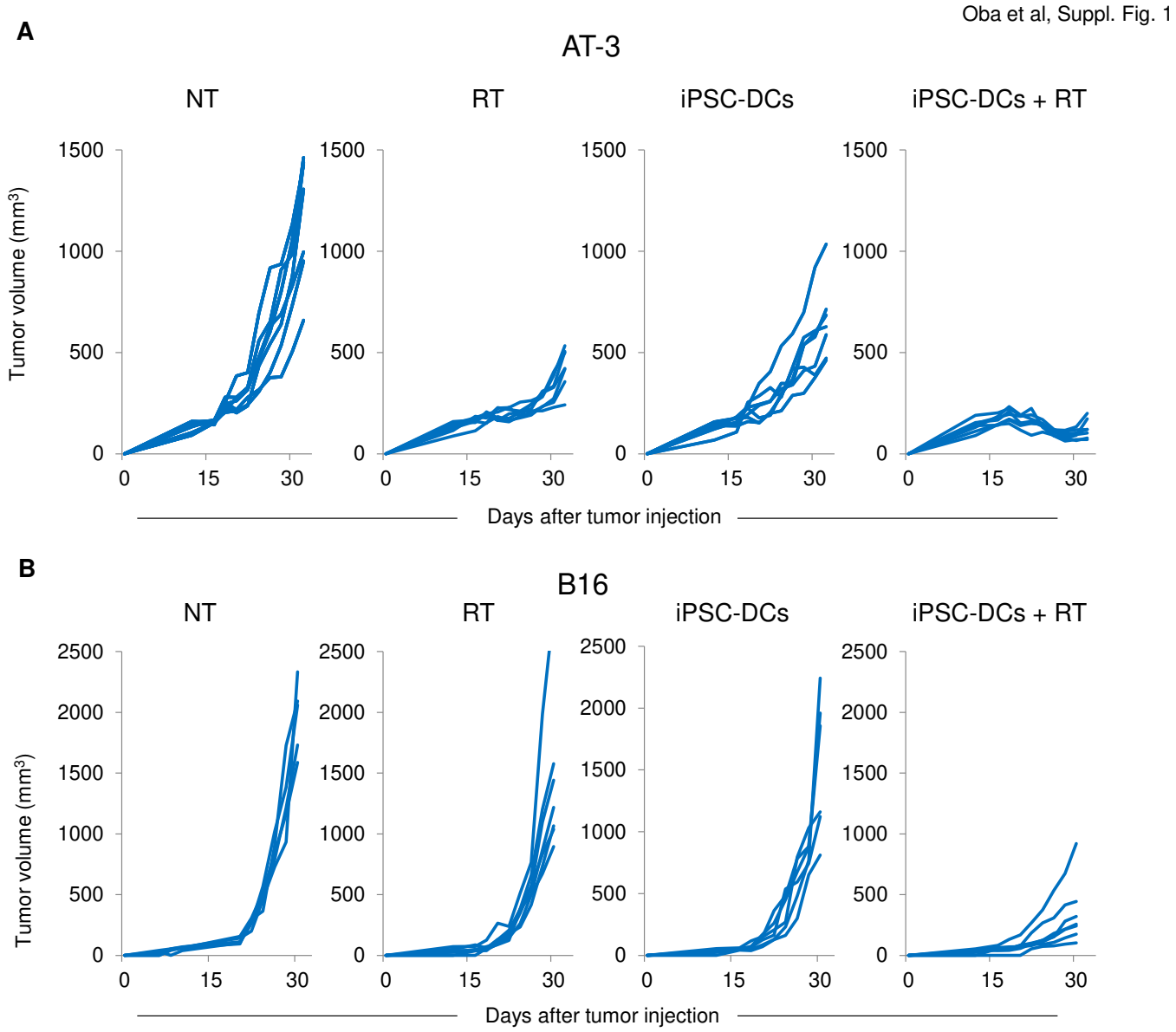

Supplementary Fig. 1 Synergistic antitumor efficacy of *in situ* administration of iPSC-derived DCs (iPSC-DCs) and local radiotherapy (RT) against poorly immunogenic tumors. Related to Fig. 3.

A, Tumor volume curves (individual) in AT-3 tumor-bearing mice in different treatment as indicated (n = 7).

B, Tumor volume curves (individual) in B16 tumor-bearing mice in different treatment as indicated (n = 6-7).

Oba et al, Suppl. Fig. 2

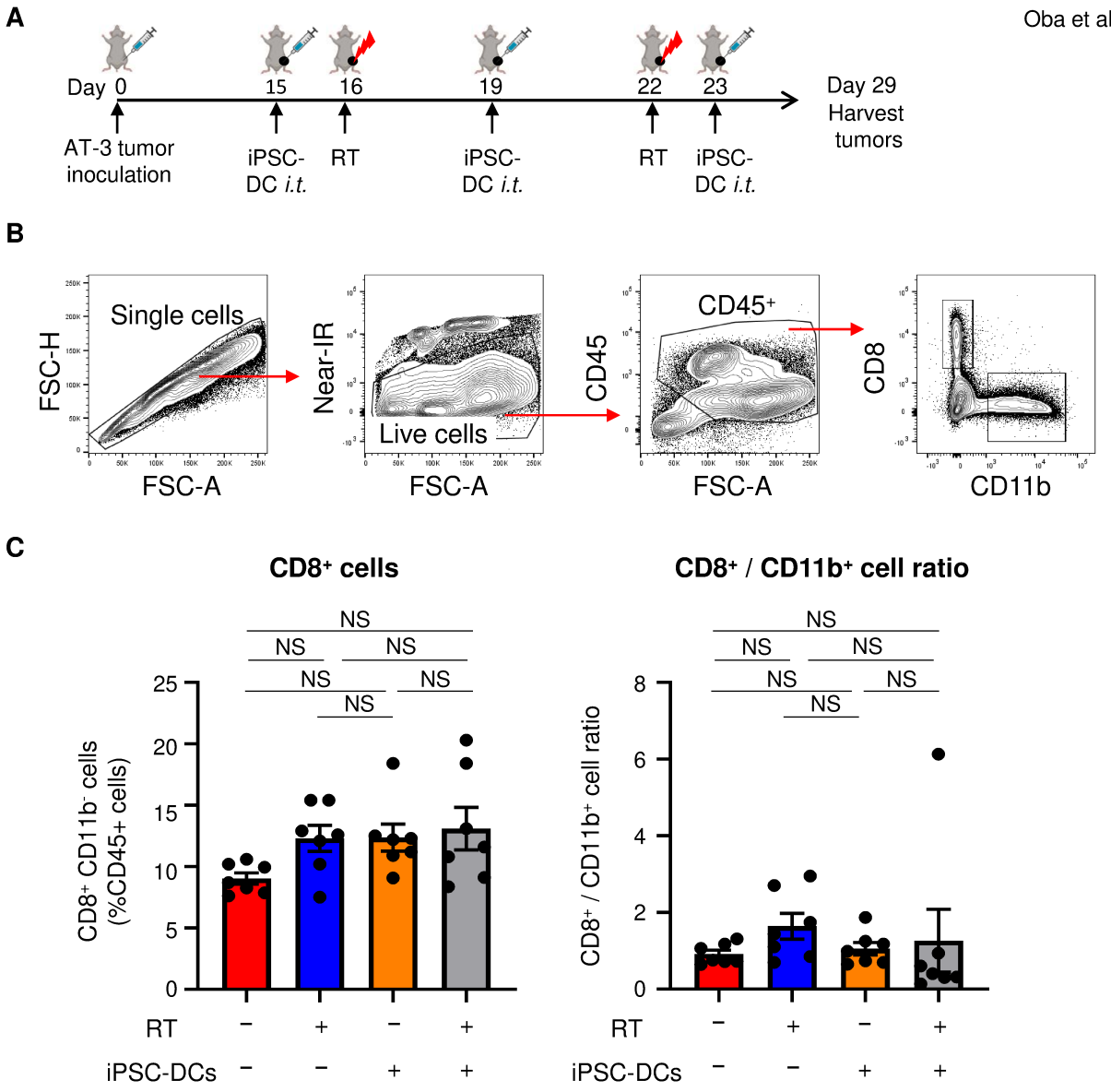

Supplementary Fig. 2 *In situ* administration of iPSC-derived DCs (iPSC-DCs) and RT did not alter the frequency of CD8⁺ cells and the CD8⁺ to CD11b⁺ cell ratio in treated tumors. Related to Fig. 4.

A, Experimental set-up.

B, Gating strategy for identifying CD8⁺ CD11b⁻ and CD8⁻ CD11b⁺ cells among CD45⁺ cells.

C, Frequency of CD8⁺ CD11b⁻ cells (left) and CD8⁺ / CD11b⁺ cell ratio (right) among CD45⁺ cells in AT-3 tumors treated with *in situ* iPSC-DC injection and/or RT. Each dot represents biologically independent mice.

NS not significant by one-way ANOVA with Tukey's multiple comparisons. Data shown are representative of two independent experiments. Mean ± SEM.

Oba et al, Suppl. Fig. 3

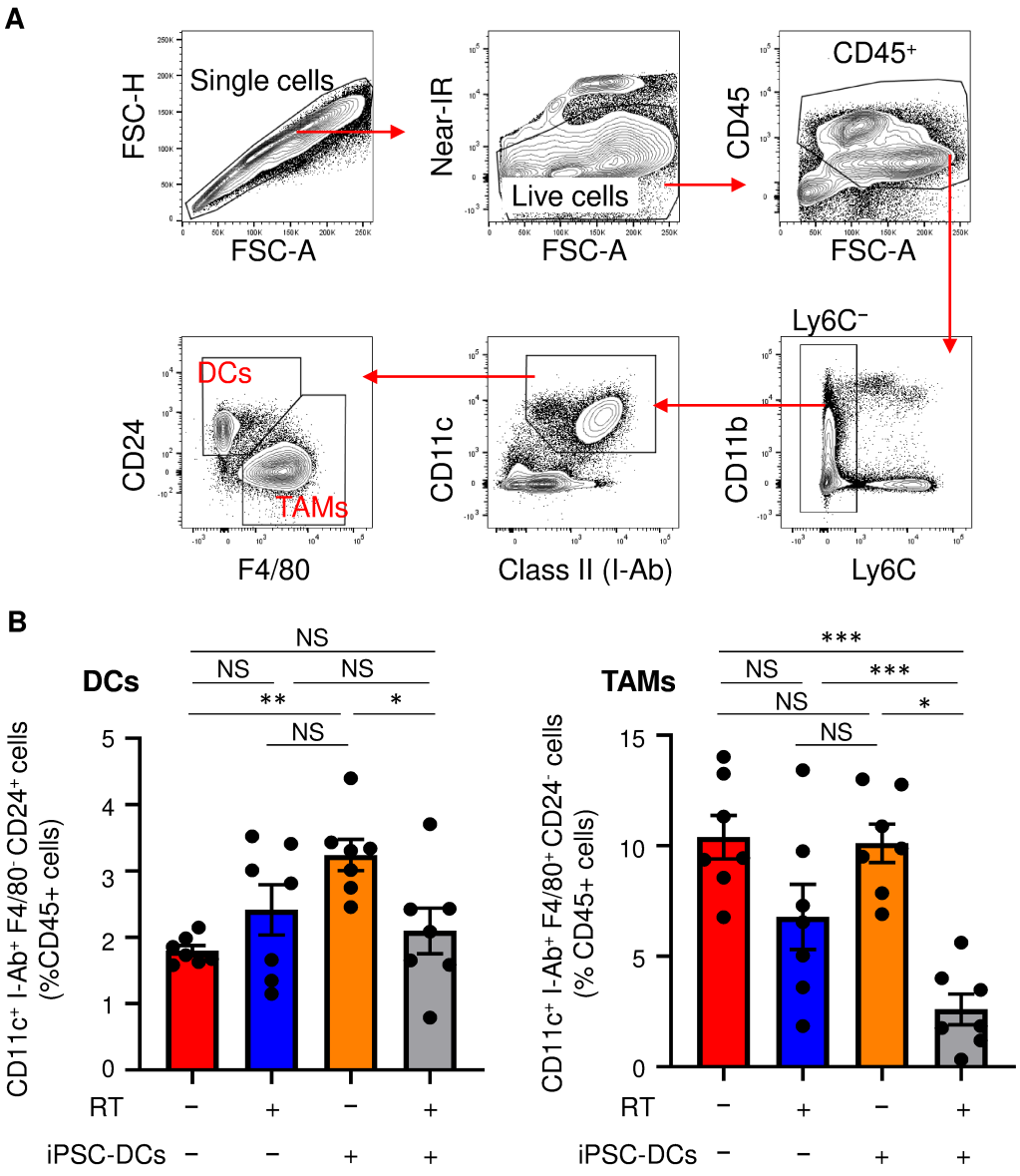

Supplementary Fig. 3 Frequency of DCs and tumor-associated macrophages (TAMs) in tumors treated with *in situ* iPSC-derived DCs (iPSC-DCs) and RT. Related to Fig. 4.

A, Gating strategy for identifying TAMs and DCs among CD45$^+$ cells.

B, Frequency of Ly6c$^-$ CD11c$^+$ class II$^+$ F4/80$^-$ CD24$^+$ DCs (left) and Ly6c$^-$ CD11c$^+$ class II$^+$ F4/80$^+$ CD24$^-$ TAMs (right) in AT-3 tumors treated with *in situ* iPSC-DC injection and/or RT. Tumors were harvested 6 days after the last injection of iPSC-DCs as described in Supplementary Fig. 2.

NS not significant, *$p < 0.05$, **$p < 0.01$, ***$p < 0.001$ by one-way ANOVA with Tukey's multiple comparisons. Data shown are representative of two independent experiments. Mean ± SEM.

Oba et al, Suppl. Fig. 4

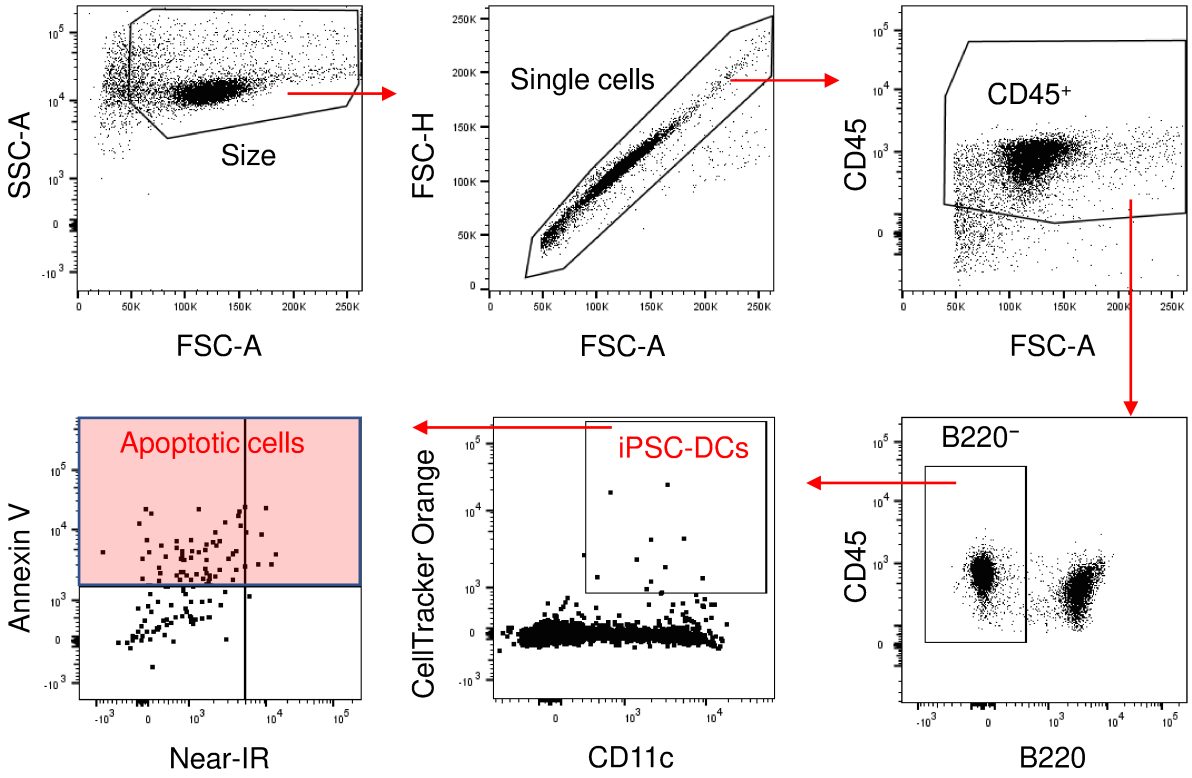

Supplementary Fig. 4 Gating strategy for identifying fluorescently-labelled iPSC-DCs and Annexin V+ iPSC-DCs among CD45+ cells in tumor-draining lymph nodes and tumors. Related to Fig. 4B, C. The percentage of viable (Annexin V−/Near-IR−), necrotic (Annexin V−/Near-IR+), early apoptotic (Annexin V+/Near-IR−) and late apoptotic (Annexin+/Near-IR+) cell populations

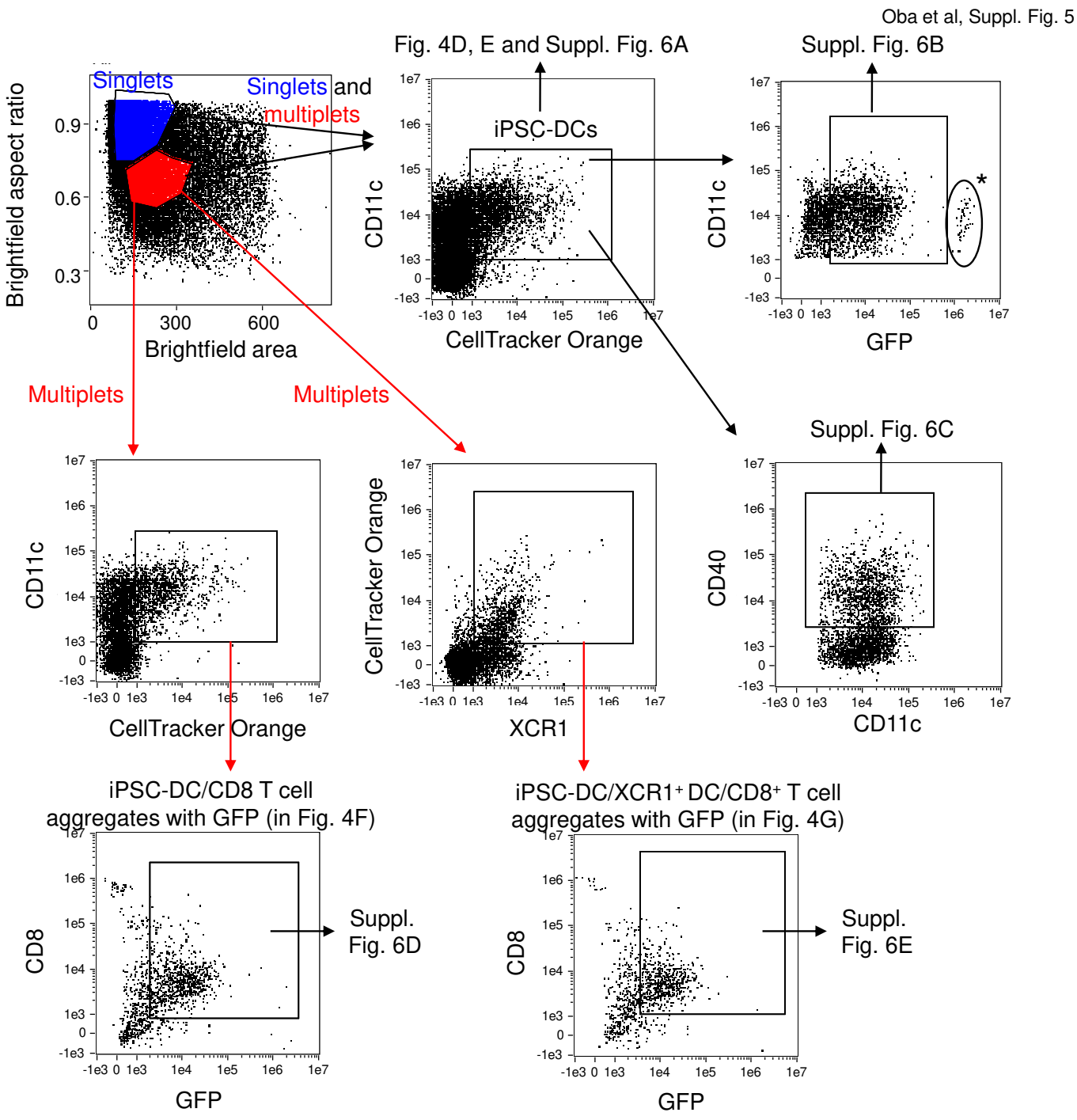

Supplementary Fig. 5 Gating strategy for identifying GFP+ iPSC-DCs, CD40-expressing GFP+ iPSC-DCs in singlets/multiplets, GFP+ iPSC-DC/CD8+ T-cell aggregates, and GFP+ iPSC-DC/XCR1+ DC/CD8+ T-cell aggregates in tumor-draining lymph nodes by Imaging flow cytometry. Related to Fig. 4D-G. Mice bearing AT-3-GFP tumors were treated with an intratumoral iPSC-DC injection (1 x 10^6 cells) and local RT (9 Gy) as described in Fig. 4A. Image analysis identified the GFP^{hi} population in * as AT-3 GFP tumor cells based on GFP distribution (whole cell distribution of signal as opposed to discreet distribution observed in DCs) and large cell size, and were therefore exclude from the analysis.

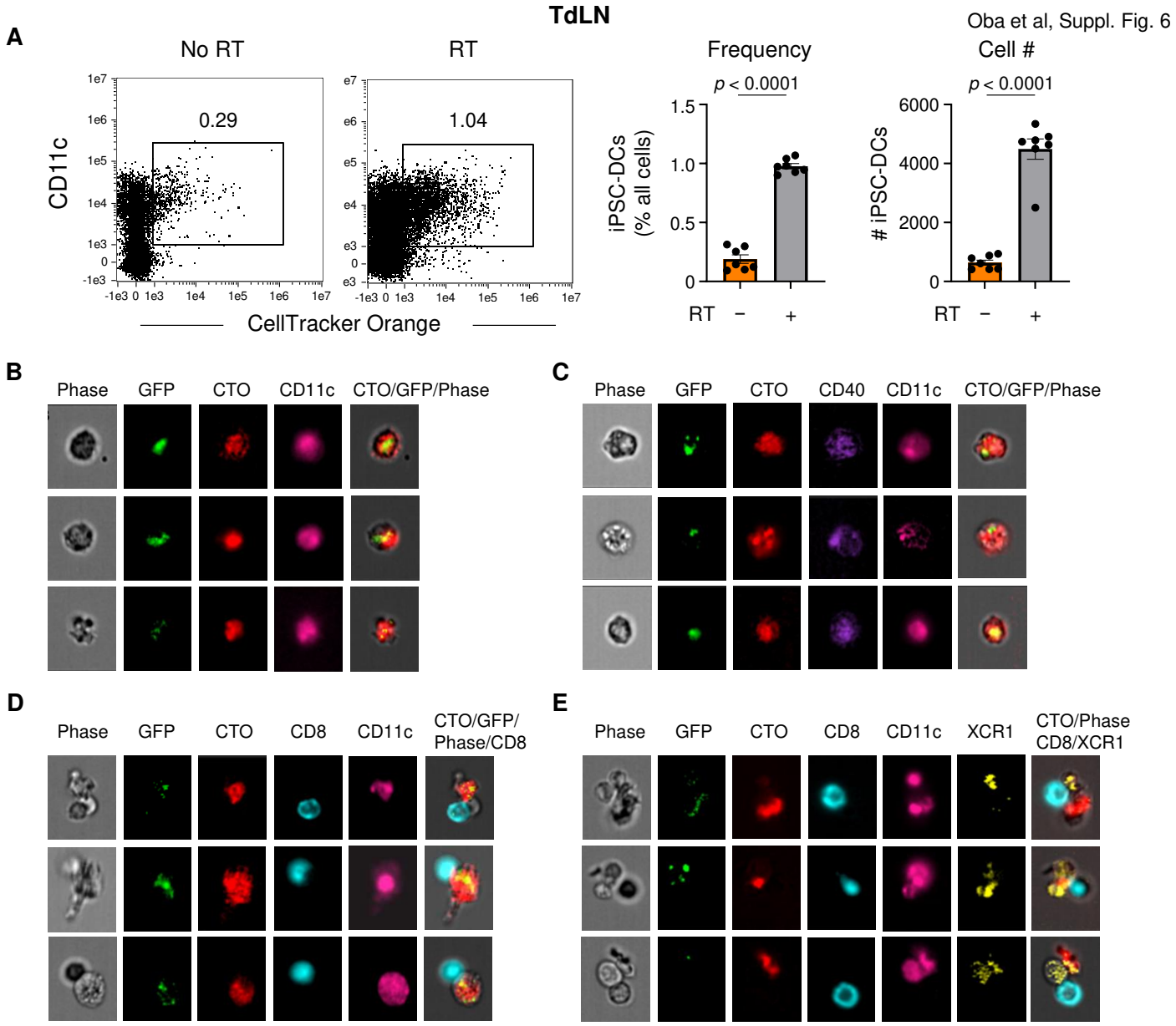

Supplementary Fig. 6 RT augments trafficking of intratumorally injected iPSC-DCs to the TdLN and increases the frequency of DC/CD8⁺ T cell aggregates. Related to Fig. 4D-G.

A-E, mice bearing AT-3-GFP tumors were intratumorally injected with 1 x 10^6 fluorescently-labelled iPSC-DCs, and were treated with or without RT. After 24 h, tumors and TdLN were analyzed for imaging flow cytometry (**Fig. 4a**). Gating strategy for each Fig. is shown in Supplementary Fig. 5.

A, Representative dot plots identifying fluorescently (CTO: CellTracker orange)-labelled iPSC-DCs. Numbers denote percent CTO⁺ CD11c⁺ cells. Data panel shows the frequency (left) and number (right) of iPSC-DCs (n = 7). Each dot represents biologically independent mice. Two-tailed student's *t*-test.

B-E, Representative images of GFP⁺ iPSC-DCs (**B**), CD40-expressing GFP⁺ iPSC-DCs (**C**) in singlets/multiplets, GFP⁺ iPSC-DC/CD8⁺ T-cell aggregates (**D**), and GFP⁺ iPSC-DC/XCR1⁺ DC/CD8⁺ T-cell aggregates (**E**). All panels in B-E are the same magnification, scale bar = 10 µm.

Oba et al, Suppl. Fig. 7

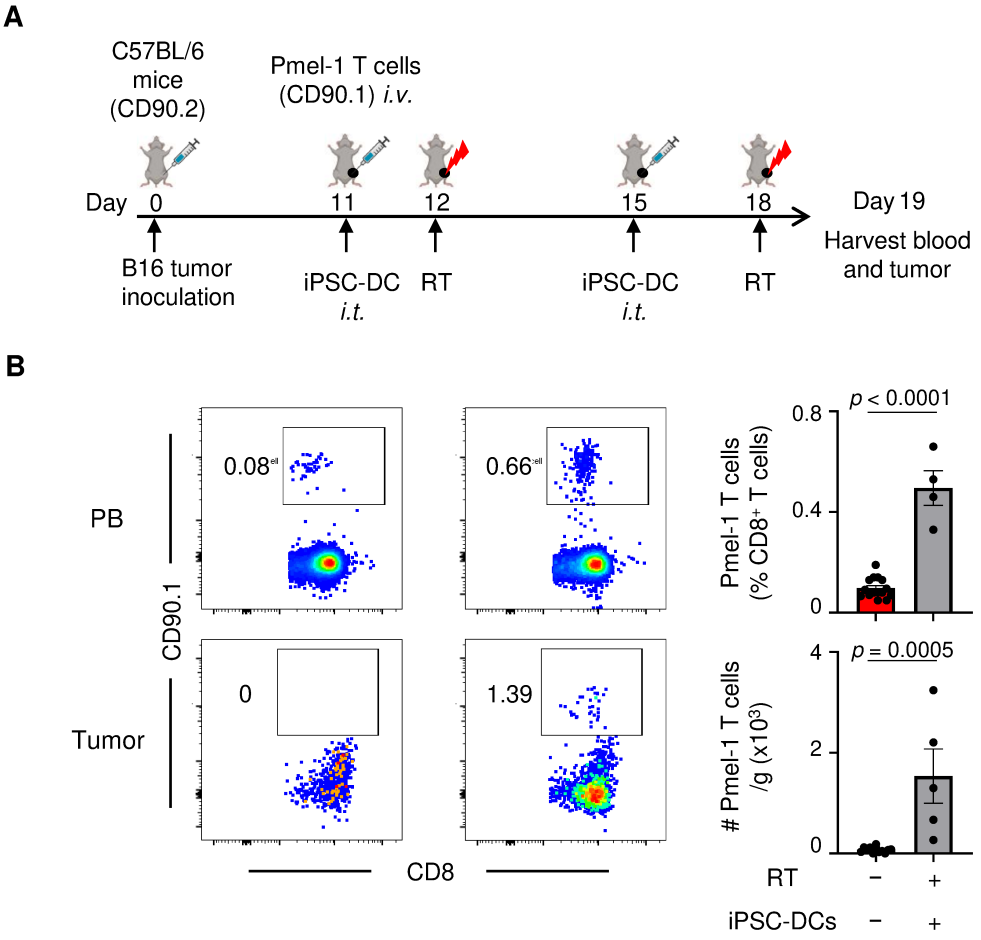

Supplementary Fig. 7 *In situ* injection of iPSC-derived DCs (iPSC-DCs) with local radiotherapy increases the frequency of antigen-specific CD8⁺ T cells in peripheral blood (PB) and the tumor. Related to Fig. 5.

A, Experimental set-up. Mice bearing B16 tumors were treated with intratumoral iPSC-DC (iPSC-DC) injection (1 x 10^6 cells) and local radiotherapy (RT) (9 Gy). Pmel-1 CD8⁺ splenic T cells (1 x 10^6 cells) were injected from tail vein on the day of the first injection of iPSC-DCs.

B, Representative flow cytometric plots and the frequency of showing Pmel-1 T cells (CD90.1⁺ CD8⁺) in CD45⁺ cells in PB and tumors. (n = 15 for control, n = 4 for treatment group). Each dot represents biologically independent mice.

NS not significant, two-tailed unpaired *t*-test. Mean ± SEM.

Oba et al, Suppl. Fig. 8

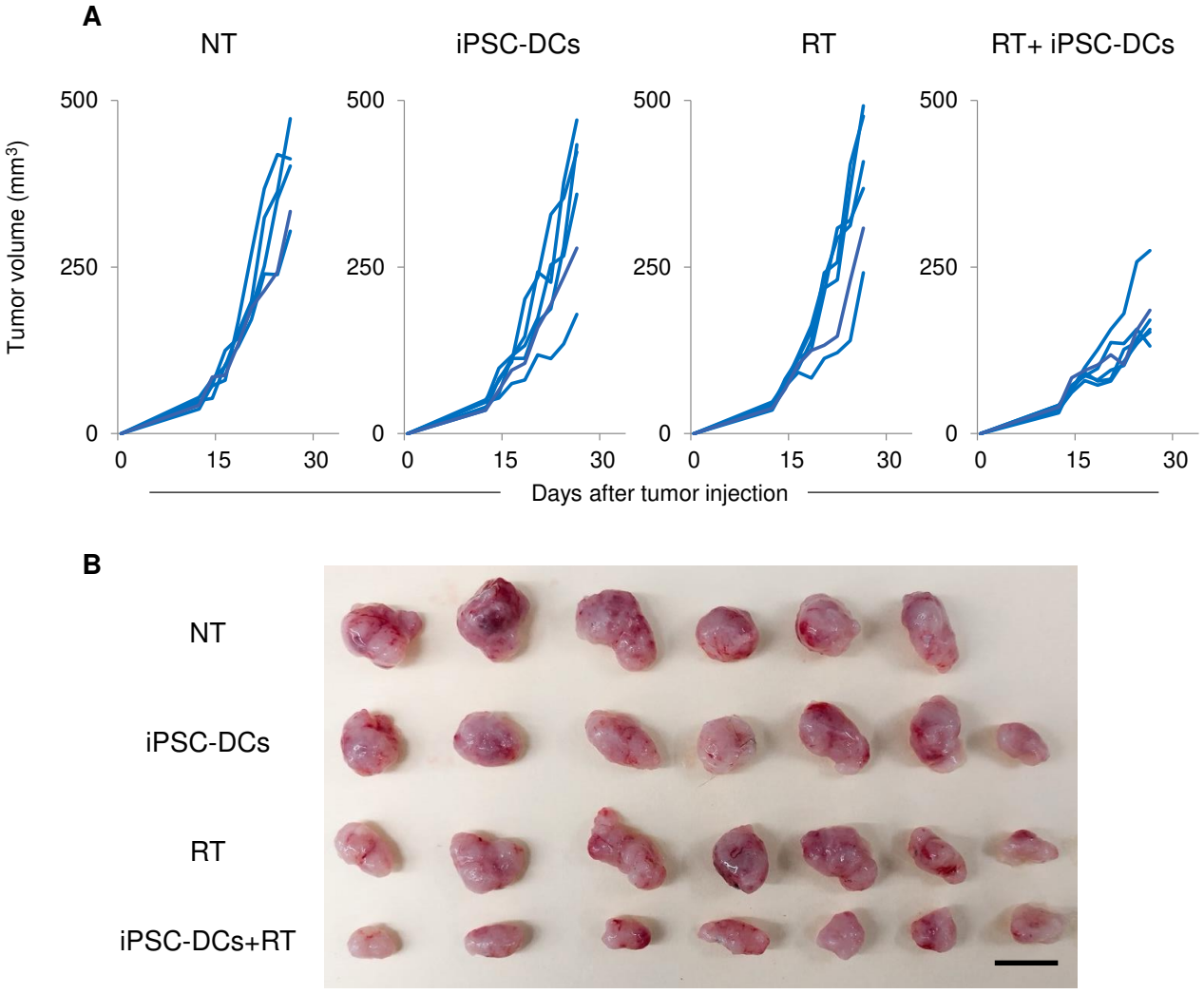

Supplementary Fig. 8 Combining *In situ* administration of iPSC-derived DCs (iPSC-DCs) with radiotherapy delays growth of distant untreated tumors. Related to Fig. 6.

A, Tumor growth curves of distant untreated tumor (individual) in bilateral AT-3 tumor-bearing mice in different treatment as to primary tumors indicated (n = 6-7).

B, Distant untreated tumors in bilateral AT-3 tumor-bearing mice in different treatment to primary tumors as indicated (n = 6-7). Scale bar, 1 cm.